Local expression of indoleamine 2,3-dioxygenase suppresses T-cell-mediated rejection of an engineered bilayer skin substitute

Farshad Forouzandeh, MD, PhD[1]; Reza B. Jalili, MD, PhD[1]; Ryan V. Hartwell, BSc[1]; Sarah E. Allan, PhD[2]; Steven Boyce, PhD[3,4]; Dorothy Supp, PhD[3,4]; Aziz Ghahary, PhD[1]

1. Burn and Wound Healing Research Laboratory, Department of Surgery,
2. Immunity and Infection Research Centre, University of British Columbia, Vancouver, British Columbia, Canada,
3. Department of Surgery, University of Cincinnati, Cincinnati, Ohio, and
4. Research Department, Shriners Burns Hospital, Cincinnati, Ohio

Reprint requests:
A. Ghahary, PhD, 351, Jack Bell Research Centre, 2660 Oak Street, Vancouver, BC V6H 3Z6, Canada.
Tel: 604 875-4185;
Fax: 604 875-4212;
Email: aghahary@interchange.ubc.ca

Manuscript received: February 19, 2010
Accepted in final form: September 1, 2010

DOI:10.1111/j.1524-475X.2010.00635.x

ABSTRACT

Engineered skin substitutes (ESSs) comprising both keratinocytes and fibroblasts can afford many advantages over the use of autologous keratinocyte grafts for the treatment of full-thickness and partial-thickness burns. In this study, we investigated the efficacy of a novel ESS containing both genetically altered fibroblasts that express the immunosuppressive factor indoleamine 2,3-dioxygenase (IDO) and primary keratinocytes from a nonautologous source to confer immune protection of xenogeneic cells cultured in a bilayer ESS. The results show that engraftment of IDO expressing skin substitutes on the back of rats significantly improves healing progression over 7 days compared with both nontreated and non-IDO-expressing skin substitutes ($p < 0.001$). Immuno-staining of CD3 and CD31 suggests that IDO-expressing skin substitutes significantly suppress T cell infiltration ($p < 0.001$) and improve neovascularization by four-fold (12.6 ± 1.2 vs. 3.0 ± 1.0 vessel-like structure/high power field), respectively. In conclusion, we found that IDO expression can improve the efficacy of nonautologous ESS for the purpose of wound healing by mitigating T-cell infiltration as well as promoting vascularization of the graft.

The skin as a multifunctional tissue provides immune defense, a barrier to external insults, as well as regulation of both heat and moisture exchange.[1] When this barrier is severely disrupted by an injury such as a burn or an ulcer, timely healing and/or repair are essential for patient survival. As in all other organs, wound healing in the skin is a dynamic process. This process involves the cooperation of platelets, fibroblasts, epithelial, endothelial, and immune cells, which together regulate a complex sequence of events that results in tissue repair.[2] The skin serves a wide range of protective, sensory, and regulatory functions. Despite the fact that many factors that promote wound healing have been identified, the topical applications of these agents have a limited value due to their short half-lives, high cost, and side effects.[3,4] As an alternative, sheets of autologous keratinocytes—first used in the clinic by O'Connor and colleagues in 1981[5]—have been used to treat patients with large thermal injuries. However, this has not been adopted as a routine procedure, as its widespread use has been hampered due to delays in obtaining the grafts, the variable acceptance rate of grafts, susceptibility of patients to infection, and high costs.[6] Moreover, cultured sheets of keratinocytes in the absence of a matrix are very fragile and are difficult to generate in patients who have a limited area of uninjured tissue as a source of primary cells. Additionally, the biopsy wounds generated to obtain the required primary cells can cause complications in patients suffering from underlying medical conditions such as diabetes, which impairs wound healing.[7] One notable shortcoming of using autologous keratinocyte sheets as a skin substitute is that there is no dermal component. Indeed, living fibroblasts play important roles in promoting keratinocyte growth, dermal–epidermal organization, and providing mechanical support to the epidermal layer.[5,8] Moreover, it has been shown that the presence of both dermal and epidermal layers allows for a highly complex ex vivo function of epidermal cells.[9] This interaction may be crucial for improved healing quality with respect to the later stages of the wound-healing process.[10] Therefore, the use of a nonautologous and readily available skin substitute that resembles full-thickness skin, comprising both dermal and epidermal cells, should significantly enhance the healing outcome in patients with severe burns and chronic wounds.[11] Although skin was the first tissue-engineered organ to be successfully developed in the laboratory, immune-mediated rejection of nonautologous skin substitutes (as with any other organ) limits the success of this wound care strategy.[1,12,13] Nonautologous skin rejection is thought to occur mostly as acute rejection and to be mainly T cell dependent.[13,14] Accordingly, the most effective immunosuppressive agents for preventing the rejection of this tissue are those that act on T cells, such as the antiproliferative drugs cyclosporine and FK506.[13,14] Although the use of immunosuppressive drugs has significantly improved the acceptance of grafts, their adverse effects reduce the quality of life in patients.[15] Therefore, the use of a targeted immunosuppressive agent that would suppress the local immune response to a

nonautologous graft without inducing unwanted systemic immunosuppression would be an ideal way to approach this problem. To this end, we hypothesized that a functional skin equivalent in which a local immunosuppressive factor such as indoleamine 2,3-dioxygenase (IDO) was expressed would improve the engraftment of a nonautologous graft without the requirement of systemic immunosuppression.

IDO is a heme-containing, rate-limiting enzyme that catalyzes tryptophan to *N*-formylkynurenine and then to kynurenine. It is primarily expressed in trophoblasts, dendritic cells, monocytes, and macrophages, whereas in other cell types, IDO is known to be an inducible enzyme.[16,17] Functional IDO is known to exert localized immunomodulatory effects on T cells as a result of the pericellular degradation of tryptophan, an amino acid required for T cell proliferation.[18–22] Indeed, IDO is important in the regulation of many different types of immune responses, such as preventing fetus rejection,[17] and in pathological conditions including neoplasia,[23,24] chronic infection,[24] asthma,[25] and autoimmune diseases.[26]

Previously, we confirmed the potential of IDO to protect engrafted xenogeneic fibroblasts propagated in collagen gel.[27] Our group has found that IDO expression in keratinocytes down-regulates their expression of cell surface major histocompatibility complex class I molecules.[28] In addition, we showed that skin cells including fibroblasts, keratinocytes, and endothelial cells, but not activated T cells, can survive and proliferate in an IDO-induced tryptophan-deficient environment.[29] This phenomenon is consistent with what has been reported for IDO-expressing trophoblasts in the placenta of a mouse model, in which bystander-infiltrated immune cells, but not trophoblast cells, were influenced by an IDO-induced tryptophan-deficient environment.[17] As a follow-up to our previous work, our aim in this study was to test the immunosuppressive function of IDO in skin substitutes containing keratinocytes, the primary immunogenic cells of the skin. We hypothesized that modified human reconstructed skin composed of both dermal and epidermal components could be modified to suppress the infiltration of T cells and prevent or delay the rejection of nonautologus grafts in rats through enforced expression of IDO. Indeed, the nonautologus skin substitute can serve not only as a temporary wound coverage but also as a rich source of cytokines and growth factors to further prepare the wound bed for the completion of the healing process by the host autologous cells.

MATERIALS AND METHODS

Fibroblasts and keratinocytes culture

All procedures were carried out following the approval of the Ethics Committee of the University of British Columbia (UBC). Neonatal foreskin pieces were used as the source of fibroblasts and keratinocytes, and cultures of human foreskin fibroblasts were established as described previously.[30] Briefly, punch biopsy samples were prepared from human foreskins. Tissue was collected in Dulbecco's modified eagle medium (DMEM; GIBCO, Grand Island, NY) with 10% fetal bovine serum (FBS, GIBCO). Specimens were dissected free of fat and minced into small pieces of < 0.5 mm in any dimension, washed with a sterile medium six times, and distributed into 60 mm$\times$15 mm Petri culture dishes (Corning Inc., Corning, NY), at four pieces per dish. A sterile glass coverslip was attached to the dish with a drop of sterile silicone grease to immobilize the tissue fragment. DMEM-containing antibiotics (penicillin G sodium, 100 U/mL; streptomycin sulfate, 100 μg/mL; and amphotericin B, 0.25 μg/mL; GIBCO) and 10% FBS were added to each dish and incubated at 37 °C in a water-jacked humidified incubator in an atmosphere of 5% CO_2. The medium was replaced twice weekly. After 4 weeks of incubation, cells were released from the dishes by a brief (5 minutes) treatment with 0.1% trypsin (Life Technologies Inc., Gaithersburg, MD) and 0.02% EDTA (Sigma, St. Louis, MO) in a phosphate-buffered saline solution (PBS; pH 7.4) and transferred to 75 cm^2 culture flasks (Corning Inc.). Once cells had grown to 90–100% confluence, the cells were subcultured 1 : 6 by trypsinization. Fibroblasts of between four and seven passages were used for this study. To culture human foreskin keratinocytes, keratinocyte serum-free medium (KSFM, GIBCO) supplemented with bovine pituitary extract (BPE, GIBCO) and recombinant epidermal growth factor (rEGF, GIBCO) was used according to the manufacturer's protocol (GIBCO). In brief, foreskins were placed into a "rinse solution" of PBS (without Ca^{2+} or Mg^{2+}) containing gentamicin (GIBCO) at a concentration of 20 μg/mL for approximately 2–3 minutes while the tissue was cut into three to four pieces of equal sizes. Each piece of tissue was then placed into a 25.0 caseinolytic units per mL solution of dispase (GIBCO) and gentamicin at 5 μg/mL. The tissues were incubated for 18 hours at 4 °C. After incubation in dispase, the epidermal layer of human keratinocytes was lifted from the dermis and placed into a 15 mL sterile centrifuge tube containing 2 mL of trypsin–EDTA (GIBCO). The tissue was incubated at 37 °C for approximately 10–12 minutes, during which time it was aspirated with a 2 mL pipette every 2–3 minutes to dissociate the cells. Following incubation, the action of the trypsin was stopped by adding 10–13 mL of soybean trypsin inhibitor (GIBCO), at a final concentration of 10 mg/mL dissolved in PBS and sterile filtered before use. The cells were spun at $149 \times g$ for 8 minutes at room temperature. The cell pellet of human keratinocytes was gently resuspended in approximately 5 mL of complete medium (i.e., KSFM containing 25 μg/mL of BPE and 0.5 ng/mL of rEGF). The primary cells were seeded into T-75 flasks at a cell density of approximately 3×10^6 cells/flask in 10 mL complete medium. Primary cultured keratinocytes of between three and five passages were used for this study.

Preparation of engineered skin substitutes (ESSs)

ESSs consisted of stratified layers of keratinocytes above dermal fibroblasts embedded within a scaffold of type I bovine collagen and glycosaminoglycan (GAG). Scaffolds were fabricated using the method previously described by Boyce et al.[31,32] using type I collagen derived from comminuted bovine hide, and chondroitin-6-sulfate without chemical cross-linking. The collagen concentration was optimized to produce a scaffold that would have a sufficient pore size to allow the migration dermal cells. Similarly, the thickness of dermal substitutes was regulated by control of the volume and concentration of starting

materials. For cell culture, the polymer substrates were rehydrated in HEPES-buffered saline solution, and changed into culture medium for inoculation of cells. For inoculation, substrates were placed on top of an *N*-terface mesh, a cotton pad, and a steel lifting platform. Transfected or primary human fibroblasts were inoculated within the collagen–GAG substrate at a concentration of $0.5\times10^6/cm^2$ and cultured at 37 °C and 5% CO_2. Medium consisting of DMEM supplemented with 5% FBS and antibiotics was used to culture human fibroblasts. For the purposes of this study, three skin substitutes (ESS) were prepared: NL-ESS, containing untransfected cells; GFP-ESS, containing GFP-transfected cells; and IDO–ESS, which contained IDO transfected fibroblasts. On the following day, the collagen–human fibroblast substrates were rinsed and incubated overnight in the skin substitute serum-free culture medium composed of the equal volume of DMEM and KSFM supplemented with antibiotics. On the next day, incubation day 0, human keratinocytes ($1.0\times10^6/cm^2$) were layered on top of the collagen–fibroblast substrates at the same side of the substrates that were inoculated previously by fibroblasts. The skin substitute culture medium was replaced daily until day 14 postincubation. Biopsies for histological evaluation were collected on days 7 and 14 for microscopic evaluations.

Adenoviral vector construction

The procedure for the construction of the IDO-expressing adenoviral (Ad) vectors has been described previously.[20] Briefly, to construct the adenovirus encoding human IDO, we cloned the PCR product encoding the full-length protein into a shuttle vector, which coexpresses GFP as a reporter gene, by following the manufacturer's instructions (Q-Biognene, Carlsbad, CA). The recombinant adenoviral plasmids were generated by electroporation of BJ5183 *Escherichia coli* of either the control shuttle vector or the vector expressing IDO. Recombinant adenoviral plasmids were then purified and transfected into 293 cells using Fugene-6 transfection reagent (Roche Applied Science, Laval, QC, Canada). Transfected cells were monitored for GFP expression, and after three cycles of freezing in an ethanol/dry ice bath and rapid thawing at 37 °C, the cell lysates were used to amplify viral particles on a large scale to prepare the adenoviral stock. Then, viral titration was carried out with the 293 cell line as described previously.[20]

Infection of fibroblasts with the Ad–GFP or the Ad–IDO–GFP vector

Recombinant adenoviruses were used to transfect fibroblasts with a multiplicity of infection of 100 as described previously.[20] Free viral particles were removed from culture media 30 hours after infection. The success of transfection was determined by fluorescence microscopy using a Motic inverted microscope (Motic Instruments, Richmond, BC, Canada) equipped with an FITC filter to view GFP-infected cells. The efficacy of transfection and the expression of functional IDO in the target cells were confirmed by analyzing the presence of IDO protein by Western immunoblotting and by measuring kynurenine levels in the conditioned media.

Kynurenine measurement in the conditioned media

We used the following assay to show IDO expression in fibroblasts that were engineered to express IDO with Ad–IDO–GFP. The biological activity of IDO was evaluated by measuring the levels of the tryptophan-degraded product, L-kynurenine, in the conditioned media from IDO-expressing cells using a previously established method.[33] Briefly, proteins in the conditioned media were precipitated by trichloroacetic acid and, after centrifugation at $9{,}000\times g$ for 5 minutes at 4 °C, 0.5 mL of the supernatant was incubated with an equal volume of Ehrich's reagent (Sigma) for 10 minutes at room temperature. The absorption of the resultant solution at 490 nm was measured using a spectrophotometer. The amount of kynurenine in the conditioned media was calculated based on a standard curve.

Protein isolation and Western blot analysis

Pieces of the NL-ESS, GFP-ESS, or IDO–ESS were weighed and cut into small pieces using a clean razor blade. Ice-cold Radio-Immuno-Precipitation Assay buffer (Sigma) was added (3 mL/g of tissue) and tissues were disrupted using a homogenizer. Next, 30 mL of 10 mg/mL of phenylmethylsulfonyl fluoride (Sigma) was added per gram of tissue and incubated on ice for 30 minutes and then spun at $14{,}000\times g$ for 20 minutes. The supernatant was retained and centrifuged again at $14{,}000\times g$ for 20 minutes. The resulting supernatant was used as the total cell lysate.

For the detection of IDO expression, the total proteins from cell lysates (20 μg/lane) were separated on 10% SDS-PAGE gels and transferred to PVDF membranes (Millipore, Bedford, MA). Membranes were probed with polyclonal rabbit anti-human IDO antibody (Washington Biotechnology Inc., Baltimore, MD) at a final dilution of 1 : 5,000. Enhanced chemiluminescence detection system (Amersham Biosciences, Little Chalfont, Buckinghamshire, UK) was used in all blots to detect the secondary HRP-linked antibody.

In vitro proliferation assay for lymphocytes

Lymphocytes were pulsed with [^{3}H]-thymidine (1 μCi/mL, Perkin Elmer, Boston, MA) on day 3 and harvested on day 4 for the measurement of [^{3}H]-thymidine by β-scintillation counting. Briefly, 74 KBq of [^{3}H]-thymidine (Perkin-Elmer Life Sciences Inc., Boston, MA) was added to each mL of the conditioned medium and the cells were incubated for 16 hours. Lymphocytes were then harvested, washed three times with PBS, dissolved in guanidium isothiocyanate, and added to scintillation fluid (Amersham Corp., Arlington Heights, IL). Radioactive counting was performed using a Beckman scintillation counter. All proliferation experiments were performed in three sets of experiments and reported as an average of counts per minute (CPM). In one control group, we added concavaline A (10 μg/mL, Sigma) to stimulate the lymphocytes before [^{3}H]-thymidine incorporation assay as a positive control group for lymphocyte proliferation.

Grafting of ESSs on Sprague–Dawley rats

Procedures on all animal studies were approved by the University of British Columbia (UBC) Animal Committee.

Before surgery, Sprague–Dawley rats (10 weeks old) were anesthetized using isoflurane. The dorsal surface of the animals was shaved and cleaned with 70% ethanol. Four full-thickness skin excision wounds were made on the dorsal surface of the rat using a 6 mm punch biopsy tool (Dormer Laboratories, Mississauga, ON, Canada). One wound was left nontreated as a control, while the other wounds were treated with either NL-ESS, GFP-ESS, or IDO–ESS. In each set of experiments, the order of treatment was changed to reduce the chance of bias in wound healing based on the place where the wounds were created on the animal. The wounds were then dressed with Tegaderm (3M, St. Paul, MN) and the grafted areas were bandaged. On day 7, the animals were euthanized and wound closure was measured and photographed. The entire wound, including a 2–4 mm margin of unwounded skin, was carefully excised. Each wound was divided into half and fixed in 4% paraformaldehyde (Fisher, Pittsburgh, PA) in PBS solution and processed for paraffin embedding.

Immuno-histochemical and immunofluorescence staining

Five-micrometer-thick sections were cut from paraffin-embedded wounds that had been treated with either NL-ESS, GFP-ESS, or IDO–ESS, and mounted on glass slides. Paraformaldehyde-fixed and paraffin-embedded sections (5 μm) were deparaffinized and hydrated by incubation in ethanol (Sigma) for 10 minutes. To retrieve cell surface antigens, a microwave oven heating pretreatment was performed before blocking with 1% bovine serum albumin (Sigma) and 10% normal goat serum (Sigma) in Tris-buffered saline (TBS, pH 7.0).

For CD3 staining, the sections were incubated with rabbit polyclonal anti-CD3 Ab (1 : 200, Abcam, Cambridge, MA) at 4 °C for 16 hours. The secondary antibody used was biotinylated goat anti-rabbit IgG (1 : 5,000, Vector Laboratories, Burlington, CA). The signal detection was carried out using the Vector VIP substrate kit (Vector Laboratories) according to the manufacturer's instructions. The slides were counterstained with methylene green for 3 minutes, dehydrated, mounted, and examined using microscopy.

For human leukocyte antigen type I (HLA-I) staining, the sections were incubated with mouse monoclonal anti-HLA-I Ab (1 : 10, Santa Cruz Biotechnology, Santa Cruz, CA) at 4 °C for 16 hours. The secondary antibody used was biotinylated goat anti-mouse IgG (1 : 500, Vector Laboratories). The signal detection was carried out using the Vector VIP substrate kit (Vector Laboratories) according to the manufacturer's instructions. The slides were counterstained with methylene green for 3 minutes, dehydrated, mounted, and examined using microscopy.

For CD31 staining, pretreated, blocked sections were incubated with mouse monoclonal anti-platelet endothelial cell adhesion molecule-1 (PECAM-1) Ab (1 : 50, Abcam) at 4 °C for 16 hours. The secondary antibody used was Alexa-Fluor 488 goat anti-mouse (1 : 4,000, Invitrogen, Carlsbad, CA). The slides were then mounted with a DAPI (4′-6-diamidino-2-phenylindole) nuclear stain containing mounting medium (Vector Laboratories). The fluorescence signal detection was carried out under a fluorescent Zeiss Axioplan 2 microscope. Northern Eclipse image analysis software was used to obtain the images.

Statistical analysis

Data were expressed as mean ± SD and analyzed using one-way ANOVA among different groups of each cell type where indicated. For post hoc testing, Student's *t*-test with Bonferroni correction for multiple comparisons was used to compare the groups. *P*-values of < 0.05 are considered statistically significant in this study.

RESULTS

IDO–ESS has an immunosuppressive activity on co-cultured nonautologous immune cells

To establish whether the adenoviral expression of IDO in IDO–ESS resulted in physiological levels of bioactive IDO enzyme, the levels of bioactive IDO in the IDO–ESS were compared with those in skin substitutes containing normal untransfected cells (NL-ESS) and GFP-transfected cells (GFP–ESS). For this purpose, we determined the levels of kynurenine, the main tryptophan metabolite of IDO activity, in the conditioned media from each of the different ESSs preparations after 72 hours of viral transfection. As shown in Figure 1A, the level of kynurenine in the conditioned medium from the IDO–ESS was significantly higher than that of either the NL-ESS or the GFP-ESS. Furthermore, Western blot results (Figure 1B) showed an intense band representing IDO protein in the cell lysate for IDO–ESS relative to that of controls.

To investigate the potential immunomodulatory role of IDO in suppressing nonautologous lymphocyte proliferation, peripheral lymphocytes were exposed to sections of skin substitutes. As shown in Figure 1C, photomicrographs suggest that the proliferation of lymphocytes was suppressed in the IDO–ESS co-culture but not in the other co-cultures, in which activated lymphocyte clusters were visible. The inhibitory effect of the IDO–ESS was markedly reversed in the presence of a specific IDO inhibitor, 1-methyl-DL-tryptophan (1-MT). To further quantify these findings, the proliferation rate of co-cultured lymphocytes was measured using the [^{3}H]-thymidine incorporation assay. The results showed almost a five-fold reduction in the proliferation of the lymphocytes exposed to IDO–ESS compared with those exposed to GFP-ESS (from 16,329.33 ± 1,785.786 CPM for GFP-ESS to 2,983.5 ± 903.72 CPM for IDO–ESS, $p < 0.001$, Figure 1D). Notably reduced lymphocyte proliferation appeared to be correlated with IDO expression, as this phenomenon could almost completely reversed upon the addition of 1-MT to this co-culture. Lymphocytes cultured for 72 hours in the absence of ESS or with concavaline A were used as negative and positive controls, respectively.

Expression of IDO improves the efficacy of ESS for wound healing of rat skin

To test whether the IDO–ESS would also have an immunosuppressive effect in vivo, we tested the efficacy of the different ESSs in a rat model of wound healing. Four skin wounds (0.282 cm^2) were made on the back of each Sprague–Dawley rat (Figure 2A). Wounds were then

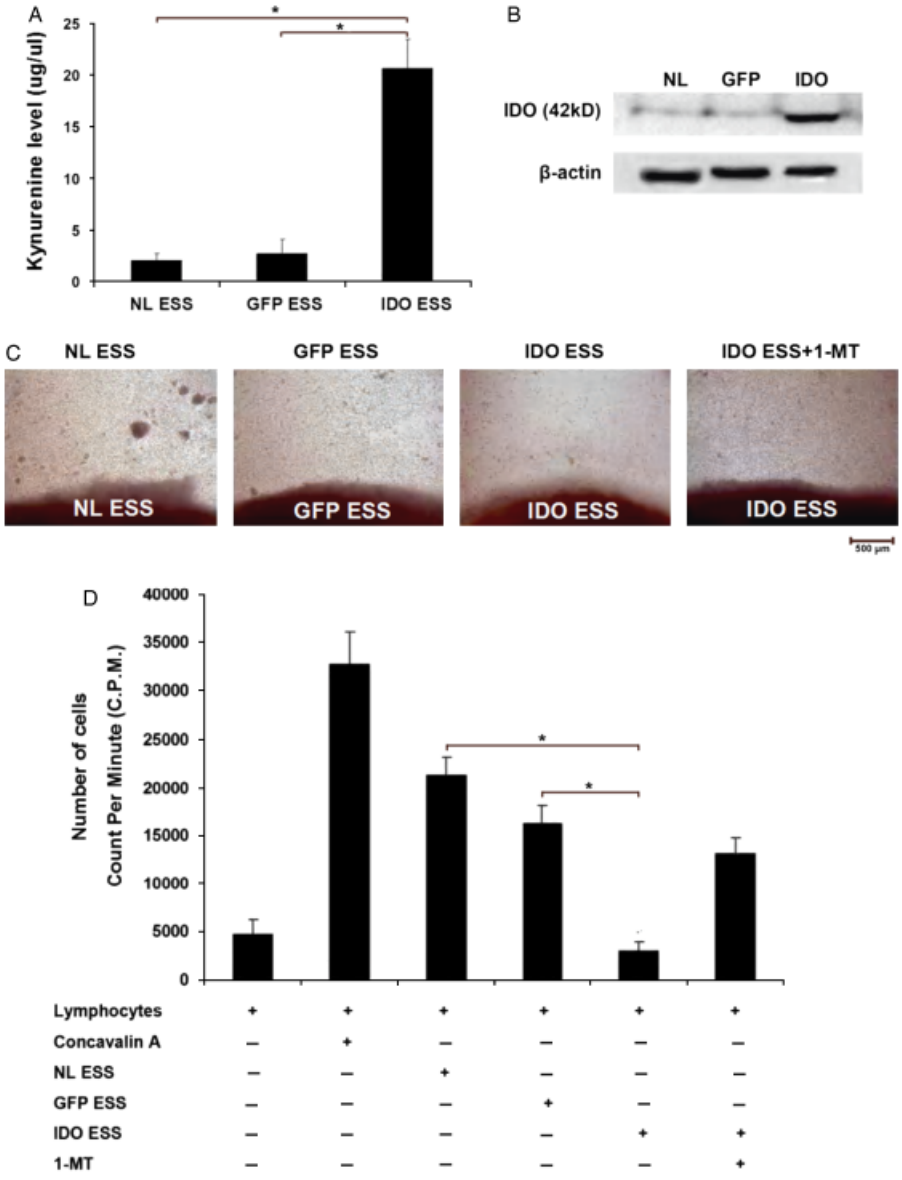

Figure 1. IDO expression and activity in ESSs. (A) Measurement of kynurenine levels in the conditioned media of NL-ESS, GFP-ESS, or IDO–ESS. Conditioned media were collected from the same number of infected and non-infected cells. (B) Expression of IDO protein was evaluated in the different ESSs by Western blot analysis. (C) An equal size of each of the different ESSs was co-cultured with 2×10^6 cells/mL rat lymphocytes for 72 hours. Photographs were taken under a light microscope. Scale bar equals 500 μm. (D) Lymphocytes were isolated from the co-culture and subjected to a [^{3}H]-thymidine incorporation assay to assess proliferative capacity. Data represent [^{3}H]-thymidine incorporation of lymphocytes co-cultured with NL-ESS, GFP-ESS, or IDO–ESS. In one set of IDO–ESS, we added 1-MT at the final concentration of 800 μM as a competitive inhibitor of IDO during the co-culture. Significant differences have been indicated by asterisks (*p-value < 0.001; $n=3$ per condition). IDO, indoleamine 2,3-dioxygenase; ESS, engineered skin substitute.

covered with either NL-ESS, GFP-ESS, or IDO–ESS, and the fourth wound was left nontreated as a control. Photographs from 7 days postwounding (Figure 2A) showed that the wound treated with IDO–ESS healed faster compared with the nontreated wound or wounds that had been treated with control ESS. The results of five sets of wounds showed that the wounds treated with IDO–ESS had an average of almost four-fold smaller surface area compared with those that received GFP-ESS ($2.9\pm1.7\,mm^2$ for IDO–ESS vs. $13.4\pm2.4\,mm^2$ for GFP-ESS, $p < 0.05$) 7 days after ESS engraftment (Figure 2B).

To evaluate wound bed histology, tissue specimens were collected on day 7 postengraftment, cross-sectioned, stained with hematoxylin and eosin, and analyzed by microscopy (Figure 2C). The histological evaluation revealed that those wounds treated with IDO–ESS were not only completely closed, but also exhibited less cellularity when compared with control ESSs (Figure 2C). This finding indicates that wounds that were treated with IDO–ESS healed faster, and possibly, with a reduced inflammatory response to the graft compared with the nontreated or control-treated wounds. Moreover, to confirm the engraftment process of the ESS cells, we stained the wound sections postengraftment for HLA-I. Immunohistochemical staining revealed HLA-positive cells in the wounds that received any of the three types of the ESS used in this study and no positive cells in the wounds that were left without any ESS engraftment (Figure 2D). As HLA-I is specific to human cells and not the rat cells,[32] any positive cells for HLA-I in these sections had to originate from the engrafted ESSs.

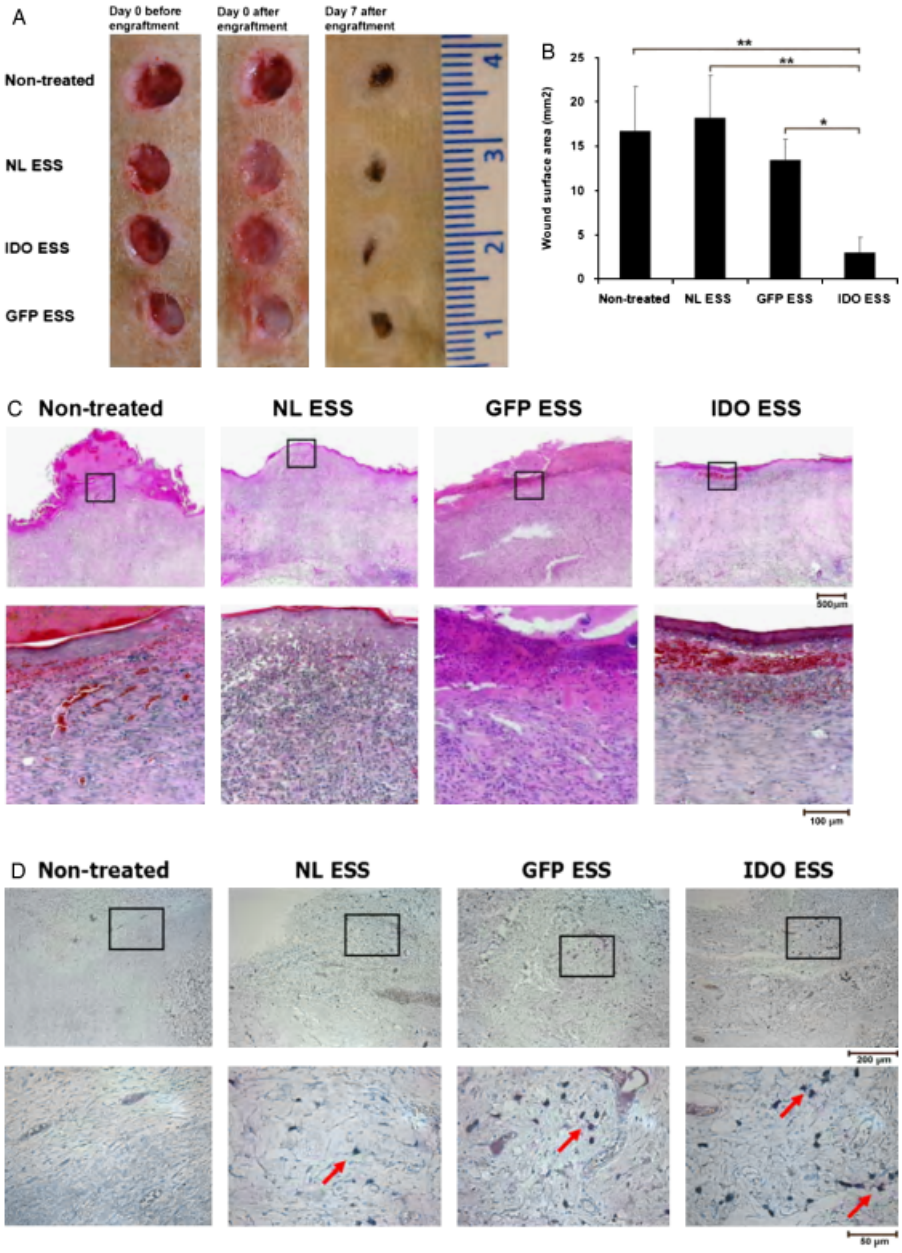

Figure 2. Degree of healing of 6 mm circular wounds treated with different ESSs. Four wounds were made on the dorsal surface of Sprague–Dawley rats using a 6 mm punch biopsy tool. Each wound was either left nontreated or treated with NL-ESS, GFP-ESS, or IDO–ESS. (A) Wounds on day 0 before and after engraftment, and at day 7 after engraftment are shown. (B) Quantification of wound healing 7 days after engraftment was determined by measuring the wound surface area. Significant differences are indicated by asterisks (*p-value < 0.05, **p-value < 0.001, $n=5$ per condition). (C) A representative hematoxylin and eosin-stained wound section on day 7 is shown. Scale bar equals 500 μm in the upper row and 100 μm in the lower row. (D) Wound sections at day 7 after engraftment were stained for HLA-I to confirm the engraftment process of ESS cells. Scale bar equals to 200 μm in the upper row and 50 μm in the lower row. ESS, engineered skin substitute; IDO, indoleamine 2,3-dioxygenase; HLA, human leukocyte antigen.

Treatment of wounds with IDO–ESS suppresses immune responses to the ESS at the site of engraftment

To evaluate the effects of the IDO expressed by the ESS on the numbers of infiltrated immune cells within the non-autologous ESSs, skin wounds ($0.282\,cm^2$) were left untreated or were treated with the different ESSs, and then harvested at day 7 postengraftment. Tissue sections from the wound were then stained for the detection of $CD3^+$ cells to analyze the degree of T cell infiltration. As shown in Figure 3A, there were fewer infiltrating $CD3^+$ T cells (per high power field, HPF) in the grafted area of the IDO–ESS-treated wounds compared with the grafts of control-treated wounds. In three experiments, the average number of infiltrating $CD3^+$ T cells in the wounds treated with IDO–ESSs was 2.5-fold lower than that of the wounds treated with GFP-ESS (32.6 ± 5.17 for the IDO–ESS group vs. 82.6 ± 18.9 for the GFP-ESS group, $p < 0.001$, Figure 3B).

IDO expression in ESS promotes neovascularization in treated wounds

It has been shown that slow revascularization is one of the causes of graft rejection for skin substitutes.[34] Therefore, we assessed whether IDO expression could promote

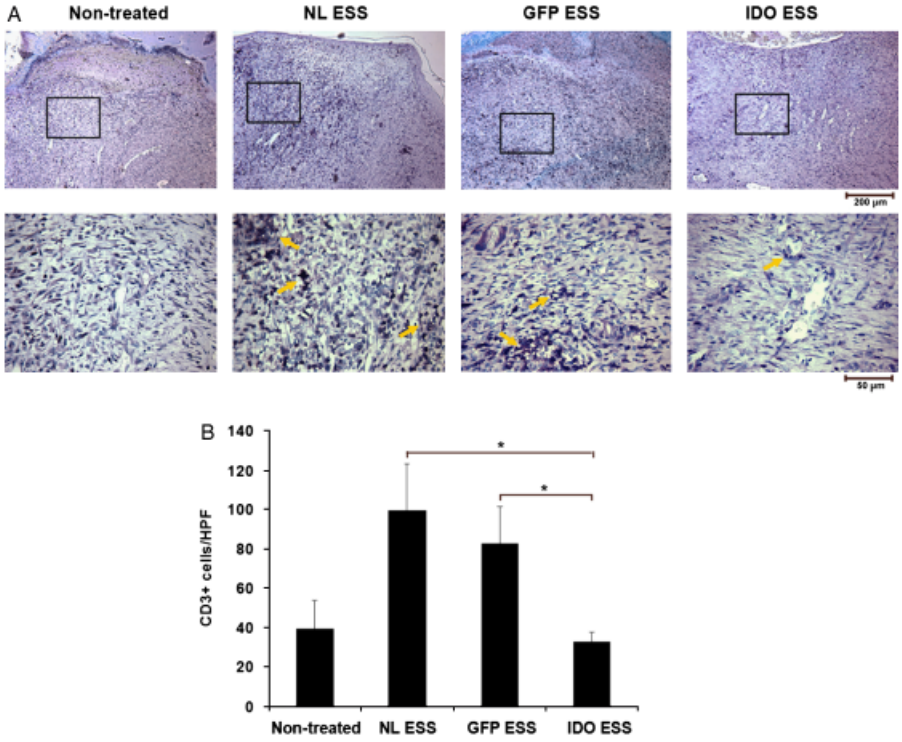

Figure 3. Detection of $CD3^+$-infiltrated lymphocytes in wound sections after engraftment. (A) Immuno-histochemical staining of $CD3^+$ T cells in sections of wounds either left nontreated or treated with either NL-ESS, GFP-ESS, or IDO–ESS 7 days after engraftment. Scale bar equals 200 µm in the upper row and 50 µm in the lower row ($CD3^+$ T cells has been shown by yellow arrows). (B) Statistical analysis of the number of infiltrating $CD3^+$ T cells per HPF at a magnification of ×400 in each wound. The significant differences are indicated with asterisks (*p-value < 0.001; $n=5$ HPF/slide; $n=3$ slides/condition). HPF, high power field; ESS, engineered skin substitute; IDO, indoleamine 2,3-dioxygenase.

angiogenesis within the ESS following engraftment. Circular wounds (6 mm or 0.282 cm^2) were treated with different ESSs or left nontreated, and then harvested at day 7 postengraftment. The sections were then stained for CD31 (PECAM-1), a marker of endothelial cells and vasculature formation.[34] As shown in Figure 4A, there were a greater number of $CD31^+$ cells and vessel-like structures in the wounds treated with IDO–ESS compared with nontreated wounds or wounds that had been treated with control ESSs. On average, the number of vessel-like structures per HPF in the wounds treated with IDO–ESS was four-fold higher than those treated with GFP-ESS (12.6 ± 1.1/HPF in the IDO–ESS group vs. 3 ± 1/HPF, in the GFP-ESS group, $p < 0.001$).

DISCUSSION

Treatment modalities for severe burns and chronic wounds continue to challenge clinicians, placing a burden on resources and patient quality of life. Advancement in tissue and biomaterial engineering has produced a variety of cellular and acellular matrix substitutes. Although many of these products provide adequate wound coverage and an environment in which cells may grow, none comprise both dermal and epidermal components.[5] More importantly, there remains a need for an for an allogeneic, patient-ready skin substitute comprising both epidermal and dermal components that will withstand antigen-specific rejection in the absence of an immunosuppression regime.[35,36] Therefore, the primary goal of this study was to develop and evaluate the functionality of an engineered skin substitute containing a stratified epidermal layer of primary keratinocytes and a dermal matrix containing IDO expressing fibroblasts in both in vitro and in vivo models. Indeed, the ability of IDO to suppress antigen-specific rejection is supported by previous evidence involving pancreatic islet,[18,22] lung,[37] and corneal[38] allografts. Moreover, we previously provided compelling evidence that both major subsets of human T cells, $CD4^+$ and $CD8^+$ T cells, are sensitive to an IDO-induced low-tryptophan and high-kynurenine environment, and that the sensitivity of T cells to this environment is due to, at least in part, GCN2 kinase (general control nonderepressible-2 kinase) activation in T cells.[19,29] Furthermore, we confirmed that using IDO as a local immunosuppressive factor has no significant adverse effect on nonimmune cells, notably keratinocytes and fibroblasts.[29] In an earlier report, we showed that IDO expression in a xenogeneic, simple collagen matrix was sufficient to provide both wound coverage and suppression of antigen-specific rejection.[27] Moving toward a more complex system including both keratinocytes and fibroblasts in a clinically approved matrix system, this study sought to examine the efficacy of IDO in protecting a multicellular graft and to address what benefit IDO may have on the wound-healing process, specifically angiogensis. To ensure successful transfection of a functional IDO gene, we measured kynurenine levels in conditioned media and evaluated the proliferation rate of lymphocytes co-cultured with nonautologous IDO-expressing (IDO–ESS) and non-IDO-expressing ESSs (NL-ESS and GFP-ESS) skin substitutes. Our results verified that IDO expression within an engineered matrix could create localized immune suppression. Confirmation of these results in vivo using Sprague–Dawley rats showed that IDO could again confer localized immune suppression for the nonautologous graft, even when containing non-IDO-expressing nonautologous keratinocytes.

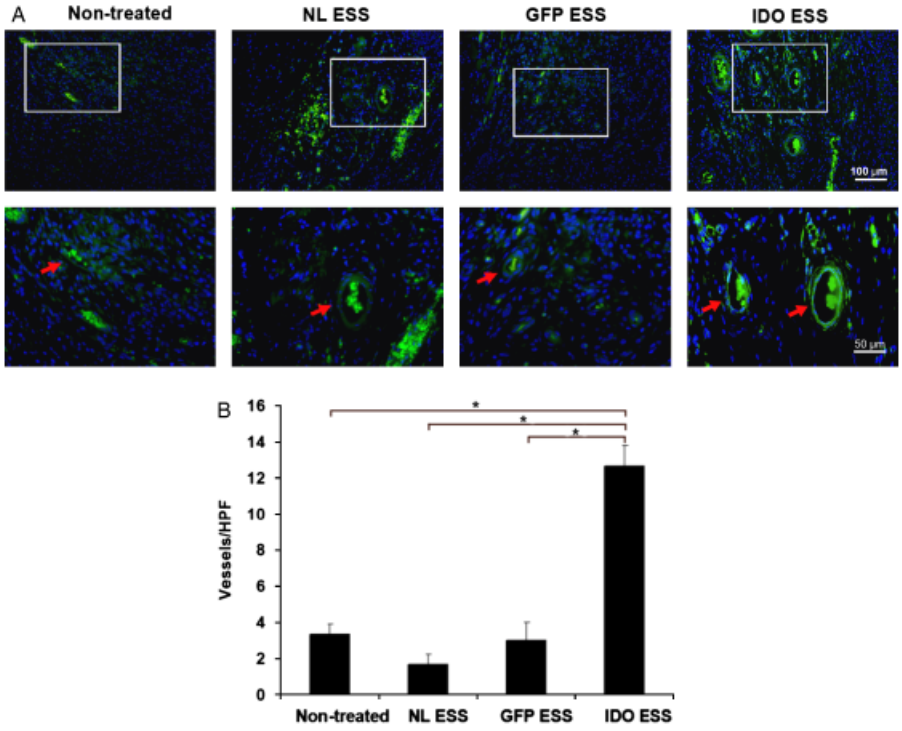

Figure 4. Detection of vessel-like structures in wound sections after treatment with ESSs. (A) Immunofluorescence staining of $CD31^+$ cells in sections of wounds left nontreated or treated with either NL-ESS, GFP-ESS, or IDO–ESS 7 days after engraftment. Scale bar equals 100 μm in the upper row and 50 μm in the lower row (vessel-like structures have been shown by red arrows). (B) Statistical analysis of the number of vessel-like structures per HPF at a magnification of ×400 in each wounds is shown. The significant differences have been indicated with asterisks (*p-value < 0.001; $n=5$ HPF/slide; $n=3$ slides/condition). HPF, high power field; ESS, engineered skin substitute; IDO, indoleamine 2,3-dioxygenase.

It has previously been proposed that IDO expression can augment localized angiogenesis,[27] which is essential for long-term graft survival. This phenomenon is analogous to the production of VEGF under conditions of hypoxia leading to neovascularization.[39] Indeed, our data further supported the role for IDO in angiogenesis, as skin substitutes expressing IDO depicted significantly more vasculature formation. Our data are the first to show the feasibility of creating a patient-ready, allogeneic skin substitute, comprising matured epidermal and dermal layers using a clinically approved dermal matrix. Application of this skin substitute system improved the rate of healing and enhanced the remodeling of a vascularized dermis following grafting in our in vivo model. Importantly, the application of an engineered skin substitute with a defined basement membrane, stratified epidermal layer, and organized dermis will reduce fluid and heat loss, and may also provide, as our findings suggest, wound-healing factors that will control healing progression. Thus, further research is required to address the other benefits of a two-component (epidermal and dermal) skin substitute system and the role of IDO within wound healing. Nonetheless, the translation of this engineered IDO expressing skin substitute to the clinic will require the development of an improved gene delivery method that is suitable for human use.

In summary, our results show that the engraftment of a nonautologous and genetically modified IDO–ESS improves the wound-healing process in rats, suppresses T cell infiltration, and promotes revascularization. To address other aspects of rejection, it will be necessary to investigate not only the long-term effects of this approach but also different phases of the wound-healing process. These findings suggest that the application of a nonautologous, IDO-expressing multicellular ESS is a promising strategy that may be further developed to create a patient-ready graft for burns and chronic wounds.

ACKNOWLEDGMENTS

Conflict of interests: The authors state no conflict of interest.

This study is supported by Canadian Institutes of Health Research (CIHR). Farshad Forouzandeh held the University of British Columbia Graduate Fellowship and the BC Innovation Council Scholarship. Reza B. Jalili, Ryan V. Hartwell, and Farshad Forouzandeh held the CIHR/MSFHR Training Award in Transplant Research. The authors are grateful to Dr. J.M. Carlin (Department of Microbiology, Miami University, Oxford, OH) for his gift of IDO cDNA.

REFERENCES

1. Supp DM, Boyce ST. Engineered skin substitutes: practices and potentials. *Clin Dermatol* 2005; 23: 403–12.
2. Hemler ME. VLA proteins in the integrin family: structures, functions, and their role on leukocytes. *Annu Rev Immunol* 1990; 8: 365–400.
3. deGraffenried LA, Isseroff RR. Wound dressings alter the colony-forming efficiency of keratinocytes in cultured sheet grafts. *Cell Transplant* 2001; 10: 749–54.
4. Greenhalgh DG. The role of growth factors in wound healing. *J Trauma* 1996; 41: 159–67.

5. Atiyeh BS, Costagliola M. Cultured epithelial autograft (CEA) in burn treatment: three decades later. *Burns* 2007; 33: 405–13.
6. Meuli M, Raghunath M. Burns (Part 2). Tops and flops using cultured epithelial autografts in children. *Pediatr Surg Int* 1997; 12: 471–7.
7. Medina A, Scott PG, Ghahary A, Tredget EE. Pathophysiology of chronic nonhealing wounds. *J Burn Care Rehabil* 2005; 26: 306–19.
8. Drukala J, Bandura L, Cieslik K, Korohoda W. Locomotion of human skin keratinocytes on polystyrene, fibrin, and collagen substrata and its modification by cell-to-cell contacts. *Cell Transplant* 2001; 10: 765–71.
9. Mitrani E, Nadel G, Hasson E, Harari E, Shimoni Y. Epithelial–mesenchymal interactions allow for epidermal cells to display an in vivo-like phenotype in vitro. *Differentiation* 2005; 73: 79–87.
10. Sawicki G, Marcoux Y, Sarkhosh K, Tredget EE, Ghahary A. Interaction of keratinocytes and fibroblasts modulates the expression of matrix metalloproteinases-2 and -9 and their inhibitors. *Mol Cell Biochem* 2005; 269: 209–16.
11. Coulomb B, Friteau L, Baruch J, Guilbaud J, Chretien-Marquet B, Glicenstein J, Lebreton-Decoster C, Bell E, Dubertret L. Advantage of the presence of living dermal fibroblasts within in vitro reconstructed skin for grafting in humans. *Plast Reconstr Surg* 1998; 101: 1891–903.
12. Funeshima-Fuji N, Fujino M, Kimura H, Takahara S, Nakayama T, Ezaki T, Li XK. Survival of skin allografts is prolonged in mice with a dominant-negative H-Ras. *Transpl Immunol* 2008; 18: 302–6.
13. He C, Heeger PS. CD8 T cells can reject major histocompatibility complex class I-deficient skin allografts. *Am J Transplant* 2004; 4: 698–704.
14. Eichwald EJ, Barstad R, Graves G. Cell-mediated hyperacute rejection. III. Genetic determinants. *Immunogenetics* 1981; 14: 351–5.
15. Tredget EE, Shankowsky HA, Pannu R, Nedelec B, Iwashina T, Ghahary A, Taerum TV, Scott PG. Transforming growth factor-beta in thermally injured patients with hypertrophic scars: effects of interferon alpha-2b. *Plast Reconstr Surg* 1998; 102: 1317–28.
16. Mellor AL, Munn DH. IDO expression by dendritic cells: tolerance and tryptophan catabolism. *Nat Rev Immunol* 2004; 4: 762–74.
17. Munn DH, Zhou M, Attwood JT, Bondarev I, Conway SJ, Marshall B, Brown C, Mellor AL. Prevention of allogeneic fetal rejection by tryptophan catabolism. *Science* 1998; 281: 1191–3.
18. Alexander AM, Crawford M, Bertera S, Rudert WA, Takikawa O, Robbins PD, Trucco M. Indoleamine 2,3-dioxygenase expression in transplanted NOD Islets prolongs graft survival after adoptive transfer of diabetogenic splenocytes. *Diabetes* 2002; 51: 356–65.
19. Forouzandeh F, Jalili RB, Germain M, Duronio V, Ghahary A. Differential immunosuppressive effect of indoleamine 2,3-dioxygenase (IDO) on primary human CD4(+) and CD8 (+) T cells. *Mol Cell Biochem* 2008; 309: 1–7.
20. Ghahary A, Li Y, Tredget EE, Kilani RT, Iwashina T, Karami A, Lin X. Expression of indoleamine 2,3-dioxygenase in dermal fibroblasts functions as a local immunosuppressive factor. *J Invest Dermatol* 2004; 122: 953–64.
21. Jalili RB, Forouzandeh F, Bahar MA, Ghahary A. The immunoregulatory function of indoleamine 2, 3 dioxygenase and its application in allotransplantation. *Iran J Allergy Asthma Immunol* 2007; 6: 167–79.
22. Jalili RB, Rayat GR, Rajotte RV, Ghahary A. Suppression of islet allogeneic immune response by indoleamine 2,3 dioxygenase-expressing fibroblasts. *J Cell Physiol* 2007; 213: 137–43.
23. Uyttenhove C, Pilotte L, Theate I, Stroobant V, Colau D, Parmentier N, Boon T, Van den Eynde BJ. Evidence for a tumoral immune resistance mechanism based on tryptophan degradation by indoleamine 2,3-dioxygenase. *Nat Med* 2003; 9: 1269–74.
24. Yoshida R, Imanishi J, Oku T, Kishida T, Hayaishi O. Induction of pulmonary indoleamine 2,3-dioxygenase by interferon. *Proc Natl Acad Sci USA* 1981; 78: 129–32.
25. Hayashi T, Beck L, Rossetto C, Gong X, Takikawa O, Takabayashi K, Broide DH, Carson DA, Raz E. Inhibition of experimental asthma by indoleamine 2,3-dioxygenase. *J Clin Invest* 2004; 114: 270–9.
26. Grohmann U, Fallarino F, Bianchi R, Vacca C, Orabona C, Belladonna ML, Fioretti MC, Puccetti P. Tryptophan catabolism in nonobese diabetic mice. *Adv Exp Med Biol* 2003; 527: 47–54.
27. Li Y, Tredget EE, Ghaffari A, Lin X, Kilani RT, Ghahary A. Local expression of indoleamine 2,3-dioxygenase protects engraftment of xenogeneic skin substitute. *J Invest Dermatol* 2006; 126: 128–36.
28. Li Y, Tredget EE, Ghahary A. Cell surface expression of MHC class I antigen is suppressed in indoleamine 2,3-dioxygenase genetically modified keratinocytes: implications in allogeneic skin substitute engraftment. *Hum Immunol* 2004; 65: 114–23.
29. Forouzandeh F, Jalili RB, Germain M, Duronio V, Ghahary A. Skin cells, but not T cells, are resistant to indoleamine 2, 3-dioxygenase (IDO) expressed by allogeneic fibroblasts. *Wound Repair Regen* 2008; 16: 379–87.
30. Sarkhosh K, Tredget EE, Li Y, Kilani RT, Uludag H, Ghahary A. Proliferation of peripheral blood mononuclear cells is suppressed by the indoleamine 2,3-dioxygenase expression of interferon-gamma-treated skin cells in a co-culture system. *Wound Repair Regen* 2003; 11: 337–45.
31. Boyce ST, Christianson DJ, Hansbrough JF. Structure of a collagen–GAG dermal skin substitute optimized for cultured human epidermal keratinocytes. *J Biomed Mater Res* 1988; 22: 939–57.
32. Boyce ST, Foreman TJ, English KB, Stayner N, Cooper ML, Sakabu S, Hansbrough JF. Skin wound closure in athymic mice with cultured human cells, biopolymers, and growth factors. *Surgery* 1991; 110: 866–76.
33. Ghahary A, Tredget EE, Shen Q, Kilani RT, Scott PG, Houle Y. Mannose-6-phosphate/IGF-II receptors mediate the effects of IGF-1-induced latent transforming growth factor beta 1 on expression of type I collagen and collagenase in dermal fibroblasts. *Growth Factors* 2000; 17: 167–76.
34. Boyce ST, Supp AP, Harriger MD, Greenhalgh DG, Warden GD. Topical nutrients promote engraftment and inhibit wound contraction of cultured skin substitutes in athymic mice. *J Invest Dermatol* 1995; 104: 345–9.
35. Erdag G, Morgan JR. Allogeneic versus xenogeneic immune reaction to bioengineered skin grafts. *Cell Transplant* 2004; 13: 701–12.
36. Llames SG, Del RM, Larcher F, Garcia E, Garcia M, Escamez MJ, Jorcano JL, Holguin P, Meana A. Human plasma as a dermal scaffold for the generation of a

completely autologous bioengineered skin. *Transplantation* 2004; 77: 350–5.
37. Liu H, Liu L, Fletcher BS, Visner GA. Novel action of indoleamine 2,3-dioxygenase attenuating acute lung allograft injury. *Am J Respir Crit Care Med* 2006; 173: 566–72.
38. Beutelspacher SC, Pillai R, Watson MP, Tan PH, Tsang J, McClure MO, George AJ, Larkin DF. Function of indoleamine 2,3-dioxygenase in corneal allograft rejection and prolongation of allograft survival by over-expression. *Eur J Immunol* 2006; 36: 690–700.
39. Liu L, Marti GP, Wei X, Zhang X, Zhang H, Liu YV, Nastai M, Semenza GL, Harmon JW. Age-dependent impairment of HIF-1alpha expression in diabetic mice: correction with electroporation-facilitated gene therapy increases wound healing, angiogenesis, and circulating angiogenic cells. *J Cell Physiol* 2008; 217: 319–27.